

## Proposal of a Set of Model Polymer Additives Designed for Confocal FRAP Diffusion Experiments

JÉRÉMY PINTE,<sup>†</sup> CATHERINE JOLY,<sup>\*,†</sup> KAREN PLÉ,<sup>‡</sup> PATRICE DOLE,<sup>†</sup> AND  
 ALEXANDRE FEIGENBAUM<sup>†</sup>

UMR FARE (INRA-URCA), Moulin de la Housse, BP 1039, 51867 Reims Cedex, France, and  
 Université de Reims Champagne Ardenne, Institut de Chimie Moléculaire de Reims, CNRS UMR  
 6229, IFR 53, UFR des Sciences exactes et naturelles, Bâtiment 18 - Europol'Agro, BP 1039,  
 51687 REIMS Cedex 2, France

The migration of additives from food packaging to food stuffs is kinetically governed by the diffusion coefficient ( $D$ ) of the additive within the polymer. Food safety authorities have recently allowed the use of mathematical models to predict  $D$ , with the additive molecular weight as a single entry parameter. Such models require experimental values to feed the databases, but these values are often scattered. To deal with this issue, a fluorescent chemically homologous series of model additives was synthesized with molecular weights ( $M_w$ ) ranging from 236 g·mol<sup>-1</sup> to 1120 g·mol<sup>-1</sup>. This set was then used to collect diffusion coefficients  $D$  through confocal fluorescence recovery after photobleaching (FRAP). This microscopic technique allows in situ packaging micro migration tests. The FRAP method was tested against results from the literature before being applied to two different model polystyrenes in a preliminary study to investigate the relationship  $D = f(M_w)$ . Our intermediate objective was to compare various experimental  $D = f(M_w)$  from our method with predictions from other mathematical or semiempirical models.

**KEYWORDS:** Food packaging; diffusion; polymer; confocal; FRAP

### INTRODUCTION

Food packaging polymers contain additives that improve their properties. Unfortunately, when these polymers are in contact with food, additives are likely to migrate into foodstuffs. Food safety authorities have thus defined positive lists of monomers and additives, which may be used to manufacture plastics. Furthermore, maximum migration limits for the use of many substances in food contact material (FCM), called specific migration limits (SML), have been established on the basis of toxicological properties ( $I$ ). These limits are enforced by producers and control authorities, who conduct migration tests (E.U. regulation 2002/72, US Food Law Act).

The migration of additives is kinetically controlled by their diffusion in the packaging material. Several physical models have described diffusion in polymers (2, 3). The characteristic parameter is the diffusion coefficient,  $D$ , of the additive in the polymeric matrix. Several easy-to-use empirical models (4, 5) can be found in the literature. The European Commission and the US Food and Drug Administration have recognized one of these, which predicts the migration of additives from food packaging (6). This model, shown in eq 1, calculates the

associated  $D^*$  of an additive, based only on its molecular weight  $M_w$ , the host polymer, and temperature of use.

$$D^* = 10^4 \cdot \exp\left(A'_p - \frac{C}{T} - 0.003M_w(45 \cdot M_w^{-1/3} - 1) - \frac{10454}{T}\right) \quad (1)$$

Equation 1 has been established by the compilation of numerous published diffusion coefficients and by appropriate statistical treatment. The parameters ( $A'_p$  and  $C$ ) (Table 1) and the numerical factors have been statistically adjusted to always overestimate the real  $D$ . This provides reassurance that despite uncertainties in predicting  $D$ , migration amounts cannot be underestimated. Moreover, the calculation of  $D$  knowing only a few parameters has made this equation a useful tool in predicting migration values (compared to physical models) or to dimension dedicated experiments (migration vs time).

Drawing such a general relationship  $D = f(M_w)$  requires a very large collection of  $D$  data to fill the database, and unfortunately, experimental data are often scattered because of the different experimental systems. This issue still merits further investigation for the following reasons:

**I. Experimental Problems.** The experimental methods used to obtain  $D$  data cannot always be compared in a straightforward manner. Some experiments were conducted by migration in a food simulant and thus also took into account interactions between polymer and simulant (e.g., swelling of the polymer

\* Corresponding author. Phone: +33 326 91 38 22. Fax: +33 326 91 39 16. E-mail: Catherine.joly@univ-reims.fr.

<sup>†</sup> UMR FARE (INRA-URCA).

<sup>‡</sup> Institut de Chimie Moléculaire de Reims.

**Table 1.** Parameters Used in Equation 1

parameters	definition
$D^*_P$	overestimated coefficient of diffusion ( $\text{cm}^2 \cdot \text{s}^{-1}$ )
$M_W$	molecular weight ( $\text{g} \cdot \text{mol}^{-1}$ )
$A'_P$	polymer specific parameter
$C$	polymer specific parameter ( $\text{K}^{-1}$ )

by the simulant). Biased  $D$  values (often overestimated) were thus obtained (7). Others used stacks of virgin films in contact with an additive source such as the Moisan test (8). When using this method, thin films with perfect contact between them are needed to allow diffusion as in a bulky film. Moreover, migration experiments can last several months for high molecular weight additives and/or barrier polymers. Therefore, choosing a convenient source, maintaining good contact, and avoiding aging remain challenging experimental issues.

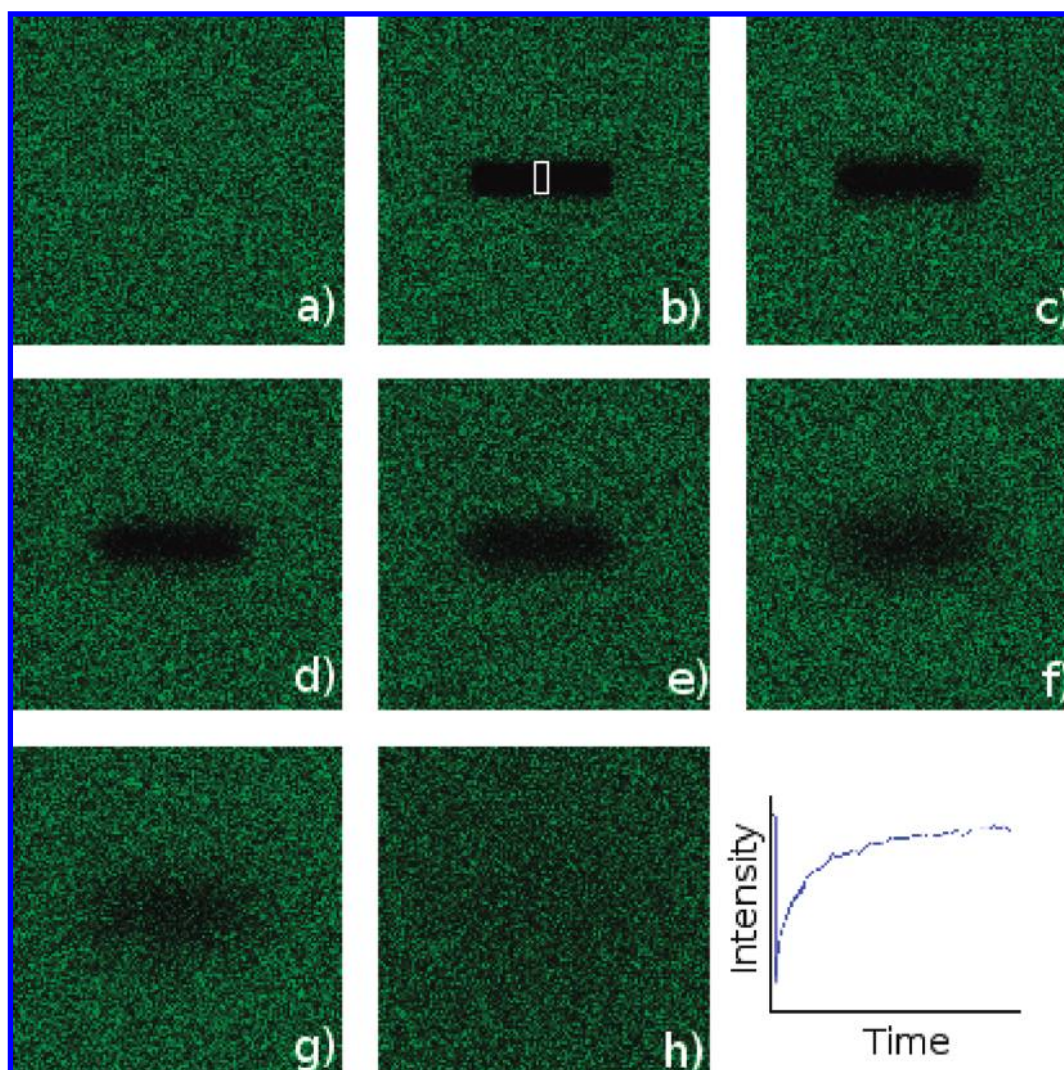
**II. Polymer Characteristics.** Barrier polymers such as polar and semipolar polymers have been much less investigated than polyolefin. For example, data compiled for eq 1 establishment initially came from polyolefin (PO) diffusion and migration reports. Now adapted for different polymers (e.g., polystyrene, polyamide, etc. (6)), the equation predicts parallel straight lines when  $\log_{10} D = f(M_W)$  curves are plotted. However, diffusion

rate versus  $M_W$  in more rigid polymers such as polyethylene terephthalate (PET) or polystyrene (PS) leads to different curve shapes than in rubbery polymers (9, 10).

**III. Migrant Characteristics.** The additives used in the compilation can be very different (steric hindrance, chemical nature, etc.), leading to scattering of the collected  $D$  data. To handle this issue, Reynier et al. (11) proposed the use of a homologous series of alkanes to determine  $D = f(M_W)$  in polypropylene (PP). Meanwhile, because of the high chemical similarity between alkanes and PO, Reynier's study is believed to give somewhat overestimated values of  $D$  and for the highest  $M_W$  items tested, and cocrystallization occurred within the PO, decreasing  $D$ .

**IV. Migrant  $M_W$ .** Molecular weight of the additives was limited, ranging from 100 to  $500 \text{ g} \cdot \text{mol}^{-1}$ , with a few samples up to  $700 \text{ g} \cdot \text{mol}^{-1}$ . High molecular weight additives were poorly evaluated except Irganox 1010 ( $M_W=1178 \text{ g} \cdot \text{mol}^{-1}$ ), which is used as a commercial antioxidant (12).

In this article, we propose an alternative methodology to collect  $D$  data based on a homologous set of model additives and fluorescence microscopy diffusion assays, to improve and investigate the useful relationship between  $D$  and  $M_W$  for additives in food packaging polymers. This is divided into two parts: (i) The interesting concept of a homologous series



**Figure 1.** Typical FRAP experiment: Diffusion of NBDNE<sub>2</sub> in PS500. The bleached ROI is  $50 \mu\text{m}$  by  $10 \mu\text{m}$ . Picture (a) was taken before bleaching, and the others were taken 2, 20, 50, 102, 252, 854, and 3104 s, respectively, after bleaching. The right corner graph depicts the evolution of fluorescence vs time (prebleach intensity, sudden loss due to bleaching, and slow recovery to initial intensity).

(repetition of the same chemical structure when increasing molecular weight) has been improved. A new homologous series has been synthesized with a larger range of  $M_w$  (from 236 to 1120  $\text{g}\cdot\text{mol}^{-1}$ ), with a structure probably closer to real polymer additives than alkanes. All components of this series are fluorescent in order to be used as diffusing species in fluorescence microscopy (see below). (ii) The use of a microscopic technique allows the observation of a microdomain of the packaging material, without simulant (or food) interactions. This offers a quick determination of intrinsic apparent diffusion coefficients of model additives, especially when dealing with low mobility matrixes. To accomplish this, we used a microscopic scale method based on confocal fluorescence recovery after photobleaching (FRAP) within the polymer. The fluorescent series was used as a set of model additives.

This article thus presents the synthesis of the set of specifically designed molecules and a complete methodology to quickly measure diffusion coefficients within polymers by confocal FRAP experiments.

## MATERIALS AND METHODS

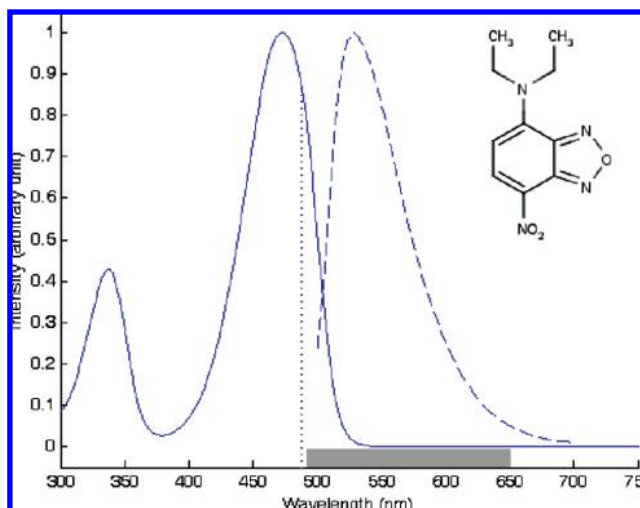
**Materials.** All reagents were reagent grade and used as supplied. Diethylamine was distilled before use. Polystyrene PS500 was obtained as a SEC standard from Sigma Aldrich (Saint Quentin Fallavier, France):  $\overline{M}_w = 514 \text{ g}\cdot\text{mol}^{-1}$ ,  $\overline{M}_n = 423 \text{ g}\cdot\text{mol}^{-1}$ ,  $\overline{M}_w/\overline{M}_n = 1.22$ . Polystyrene PS800 was purchased from Pressure Chemicals (Pittsburgh, USA):  $\overline{M}_w = 800 \text{ g}\cdot\text{mol}^{-1}$ ,  $\overline{M}_n = 667 \text{ g}\cdot\text{mol}^{-1}$ ,  $\overline{M}_w/\overline{M}_n = 1.20$ . Sucrose, used as a reference material for  $D$  measurement (12), was bought in a local supermarket.

**Synthesis and Characterization of NBD-Based Probes.** The method used to synthesize NBD-based probes is presented in Results. All specific directions for chemical synthesis and product characterization can be found in Supporting Information.

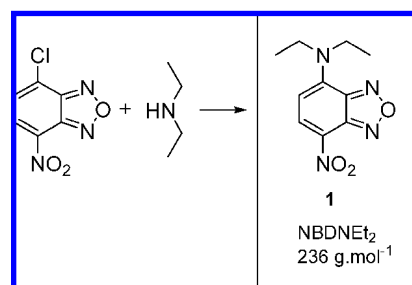
Analytical thin-layer chromatography (TLC) was performed on E. Merck Silica Gel 60 F254 plates. Compounds were visualized either by observation under a UV lamp ( $\lambda = 254 \text{ nm}$ ) or by dipping in an phosphomolybdic acid solution in ethanol and heating. NMR spectra were recorded in deuterated chloroform, unless otherwise stated, using a Bruker Advance DRX 500 spectrometer (500 MHz for  $^1\text{H}$  and 125 MHz for  $^{13}\text{C}$ ). Mass spectra were obtained by ESI MicroTOF (Q) spectrometer. Absorption and fluorescence spectra were acquired, respectively, with a Shimadzu UV-visible spectrometer ( $8.5 \cdot 10^{-4} \text{ mol}\cdot\text{L}^{-1}$  in ethyl acetate at room temperature (RT)) and a Perkin-Elmer LS50B luminescence spectrophotometer ( $2.1 \cdot 10^{-7} \text{ mol}\cdot\text{L}^{-1}$  in ethyl acetate at RT).

**Film Preparation.** Polystyrene films doped with a fluorescent probe were made by dissolving a known amount of polystyrene in an ethyl acetate solution of the fluorescent probe ( $10^{-10} \text{ mol}$  per mg of polystyrene). Approximately  $10 \mu\text{L}$  of solution were allowed to dry on a cover slide ( $22 \times 22 \text{ mm}$ ,  $150 \mu\text{m}$  thick, Menzel-Glaser) at RT and ambient atmosphere for several hours. Traces of solvent were removed by heating the cover slides in a dynamic vacuum oven at  $60 \text{ }^\circ\text{C}$  for at least one hour. The cover slides were then mounted onto a microscope slide (Menzel-Glaser SuperFrost) by slight pressure under a heating press set at  $120 \text{ }^\circ\text{C}$ . Fluorescein-doped solutions of sucrose were made by dissolving the necessary amount of sucrose into an aqueous solution of fluorescein (fluorescein concentration,  $3 \mu\text{M}$  and sucrose weight fraction, 68.5%, as described in ref 13). The sample was made by casting  $10 \mu\text{L}$  of the sucrose solution onto a microscope slide, then covering with a cover slide. In order to maintain good contact between the sample and slides, each sample had its borders sealed with nail polish.

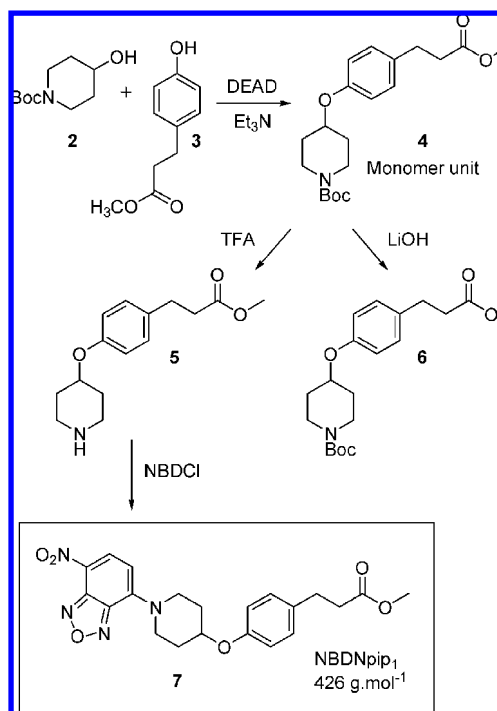
**FRAP Experiments.** FRAP is a micrograting technique first described by Axelrod (14) and then applied to the polymer field (15). A selected region of interest (ROI) of a labeled sample is selectively darkened by photooxidation of the fluorescent probes under high intensity laser illumination. The same laser, but highly attenuated, is then used to monitor fluorescence recovery into the bleached ROI



**Figure 2.** Absorption (solid line) and emission (---) spectra of NBDNEt<sub>2</sub> (respective concentrations in ethyl acetate:  $8.5 \cdot 10^{-4}$  and  $2.1 \cdot 10^{-7} \text{ mol}\cdot\text{L}^{-1}$ ). The wavelength of the CLSM laser used (· · ·) and wavelength range collected by the detector (grayed zone) are reported on the graph.



**Figure 3.** Synthesis of the first probe: NBDNEt<sub>2</sub>.



**Figure 4.** Synthesis of monomer 4 and NBDNpip<sub>1</sub> (7).

(**Figure 1**). This recovery occurs by diffusion of unbleached molecules from the surroundings into this region (16). The selection of the ROI can be made by interference of the lasers creating an interference fringe pattern (13, 15) or with confocal laser scanning microscopes (CLSM)

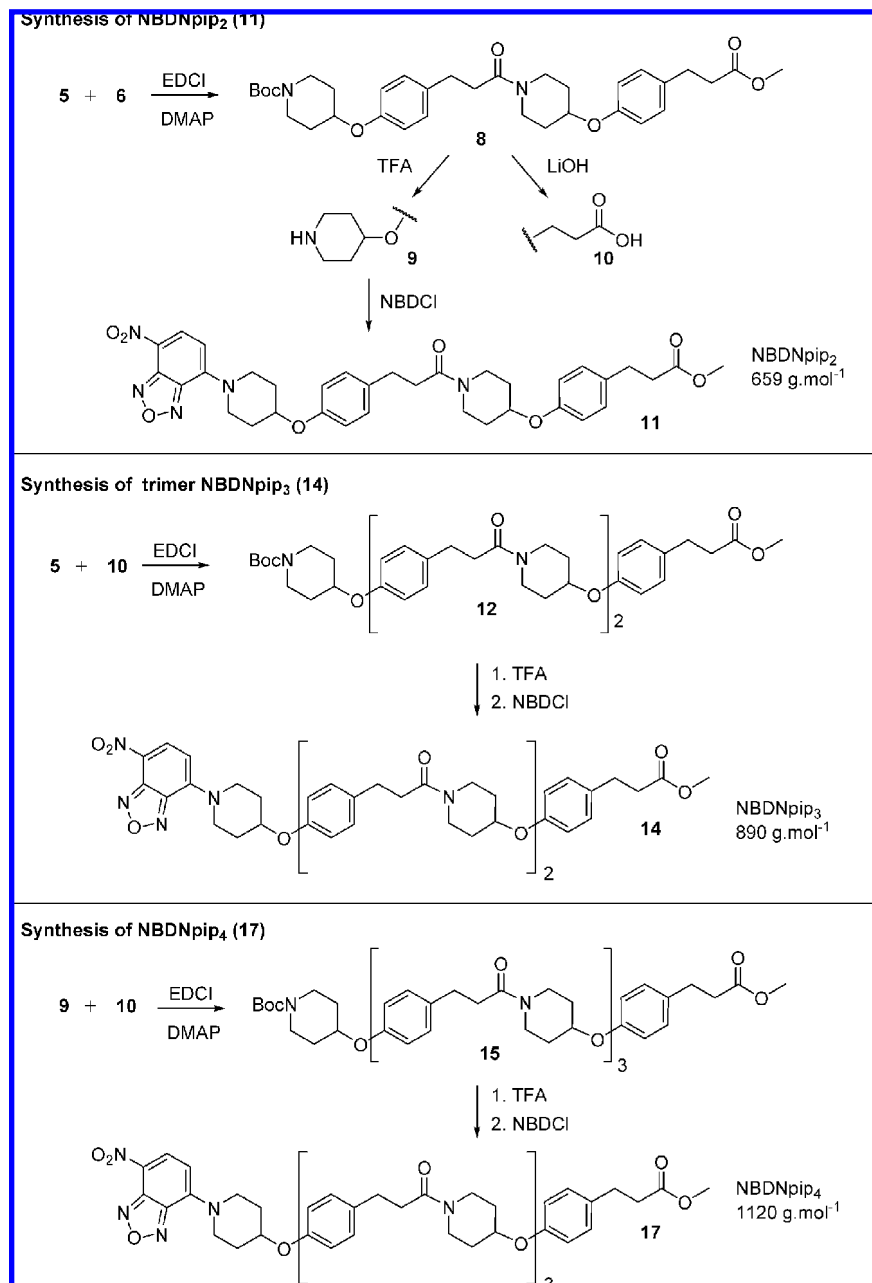

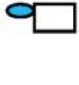

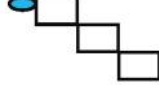
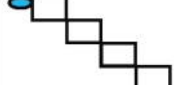
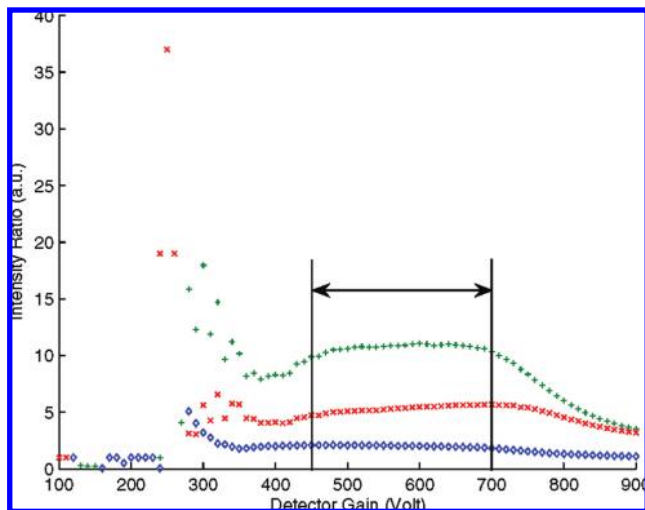


Figure 5. Synthesis of NBD oligomers.

Table 2. Characteristics of the Homologous Fluorescent Set of Model Additives<sup>a</sup>

Name	NBDNEt <sub>2</sub>	NBDNpip <sub>1</sub>	NBDNpip <sub>2</sub>	NBDNpip <sub>3</sub>	NBDNpip <sub>4</sub>
n (number of monomer units)	0	1	2	3	4
Structure scheme / compound number (Figures 3,4, and 5)					
M <sub>w</sub> (g.mol <sup>-1</sup> )	(1) 236	(7) 426	(11) 658	(14) 889	(17) 1120

<sup>a</sup> The filled elliptical head and open rectangles represent the NBD chromophore and repeating units, respectively.



**Figure 6.** Comparison of fluorescence intensity with chromophore concentration vs detector gain. NBDNpip<sub>2</sub> in PS500. Ratio of intensities: (+)  $5 \cdot 10^{-10} \text{ mol} \cdot \text{mg}^{-1}$  vs  $0.5 \cdot 10^{-10} \text{ mol} \cdot \text{mg}^{-1}$ , (x)  $2.5 \cdot 10^{-10} \text{ mol} \cdot \text{mg}^{-1}$  vs  $0.5 \cdot 10^{-10} \text{ mol} \cdot \text{mg}^{-1}$ , (◇)  $5 \cdot 10^{-10} \text{ mol} \cdot \text{mg}^{-1}$  vs  $2.5 \cdot 10^{-10} \text{ mol} \cdot \text{mg}^{-1}$ .

by drawing a selected region on the sample. This method is not restricted to confocal microscopy, as conventional light microscopy can also be used (17), but the enhancement of lateral resolutions in confocal microscopes is very useful (up to 246 nm of lateral resolution with our system). For our studies, CLSM was used to bleach thin rectangles to monitor probe diffusion over 1D. For each experiment, the fluorescence recovery was monitored in a small rectangle (length  $< 1/10$  ROI length, i.e., the white rectangle drawn in **Figure 1b**). The fluorescence recovery was therefore observed over a smaller region than the whole ROI, thus eliminating border effects.

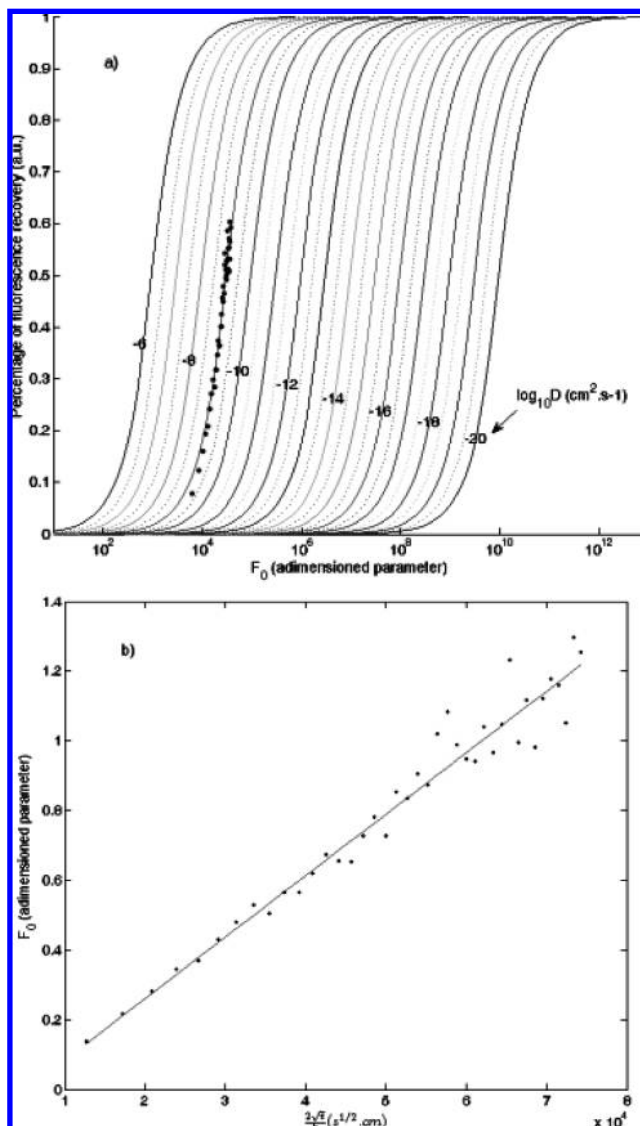
**Confocal Imaging.** The polymer films were observed using a confocal microscope Leica TCS-SP2 (Leica, Manheim, Germany), using the 20 mW- and 488 nm-line of an argon laser, and a  $63\times$  oil-immersion objective. Optical zoom was 1.9 unless otherwise stated in the text. The reflected fluorescent light was selected through a pinhole of 1 Airy. Acousto-optical tunable filters (AOTF) selected light from 492 to 650 nm (cf. **Figure 2**). Reading was performed at minimal power (approximately 0.75% of maximal power), whereas grating or photobleaching was performed under high illumination power (ca. 90% with the help of the 476 and 496 nm lines at full power). Confocal pictures are known to have a bad signal-to-noise ratio (18, 19). In order to improve this, acquisitions were performed with 2 time line averaging. FRAP experiments were repeated at least four times.

**Analysis of Confocal FRAP Kinetics.** Analysis of picture stacks was made through ImageJ (<http://rsb.info.nih.gov/ij/>), with use of StackReg plug-in (<http://bigwww.epfl.ch/thevenaz/stackreg/>). To improve picture quality, the stacks were filtered by a 2-by-2 median filter, before any analysis. To eliminate laser power fluctuations (20), the recovery curve was normalized by the background intensity. The recovery data was worked up through a laboratory-made Matlab function. More information about the mathematical background for the analysis can be found in the Results section.

## RESULTS

This section deals successively with the characteristics and synthesis of the homologous probe series, followed by their use in the FRAP methodology, and finally with the very first collected data used to draw the  $D = f(M_w)$  curve.

**Homologous Fluorescent Probe Synthesis for Confocal Experiments.** To fulfill the requirements of this study, the fluorescent component of the synthetic probes was chosen to meet certain criteria. The excited chromophore must be easily photobleached by the excitation laser of the microscope. The sensitivity to photooxidation must not be too high so as not to

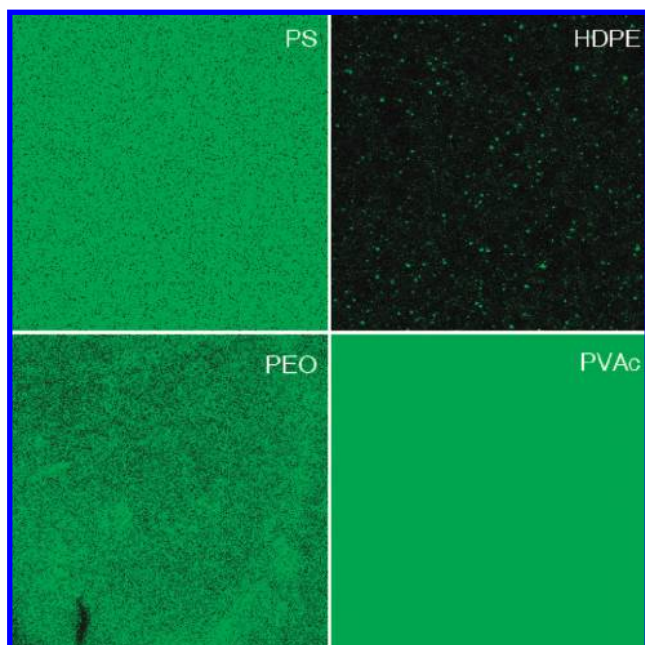


**Figure 7.** (a) Normograph drawn with the help of the equation and fluorescence recovery from the diffusion of NBDNpip<sub>1</sub> in PS500 at RT. (—) units; (· · ·) half-units, (●) data from diffusion of NBDNpip<sub>1</sub> in PS500. (b) Least mean square regression to determine the precise value of  $D$ : the graph presents results from the diffusion of NBDNpip<sub>1</sub> in PS500; corresponding  $D$  is  $1.7 \cdot 10^{-9} \text{ cm}^2 \cdot \text{s}^{-1}$ .

**Table 3.** Diffusion Coefficients ( $\text{cm}^2 \cdot \text{s}^{-1}$ ) of the Different Model Additives in PS500 and PS800 at RT

polymer	NBDNET <sub>2</sub>	NBDNpip <sub>1</sub>	NBDNpip <sub>2</sub>	NBDNpip <sub>3</sub>	NBDNpip <sub>4</sub>
PS500	$5.4 \cdot 10^{-9}$	$1.7 \cdot 10^{-9}$	$4.5 \cdot 10^{-10}$	$4.0 \cdot 10^{-10}$	$1.4 \cdot 10^{-10}$
PS800	$4.9 \cdot 10^{-11}$	$8.4 \cdot 10^{-12}$	$1.2 \cdot 10^{-12}$	$8.9 \cdot 10^{-13}$	$3.9 \cdot 10^{-13}$

be bleached when reading at low laser power. Unwanted photooxidation when reading must not interfere with fluorescence recovery. In order to have Fickian diffusion, the probe molecule must be soluble in the studied polymers. Its fluorescence yield must also be efficient at low concentration. The apolar 7-nitro-1,2,3-benzoxadiazole (NBD) core (see **Figure 2**) was chosen as the best candidate. It has been previously described in confocal FRAP experiments in apolar systems (21, 22). This molecule has numerous advantages against other well-known confocal chromophores: (i) photostability at low power, (ii) high yield of photobleaching at high power, (iii) tunability of its absorption and emission spectra (23, 24), and (iv)



**Figure 8.** Pictures of NBD probes dispersed in polymeric matrices. Spotty pictures depict nonhomogenously doped polymers. HDPE, high density polyethylene; PEO, polyethylene oxide; PS, polystyrene; PVAc, poly(vinyl acetate).

**Table 4.** Theoretical Limits of the Presented Method, Using a Leica TCS-SP2

	lower limit	upper limit
objective	63X	10X
zoom	4×	1×
time lapse	several months	0.19 s
% of fluorescence recovery	9%	50%
theoretical associated $D$	$4 \cdot 10^{-18} \text{ cm}^2 \cdot \text{s}^{-1}$	$6 \cdot 10^{-4} \text{ cm}^2 \cdot \text{s}^{-1}$

photooxidation leading to an irreversible loss of fluorescence. We did not notice any quenching of NBD fluorescence such as those reported by Braeckmans for fluorescein (19).

The first probe used in the series (NBDNET<sub>2</sub> (1)) was obtained by reaction of diethylamine and NBD chloride (Figure 3) as previously described in the literature (25). To create a series of oligomers with one to four repeating units, a pseudo amino acid monomer was chosen in order to use peptide coupling techniques to assemble the desired oligomers. The monomer unit (4) containing a protected secondary amine at one end, and a carboxylic ester at the other was synthesized by a Mitsunobu reaction between the Boc protected hydroxypiperidine (2) and the phenol (3) in good yield (Figure 4). Selective deprotection of the amine, followed by coupling with NBD chloride then gave the second probe of the series (7).

A three step reaction sequence was used to assemble the other molecules in the series. First, deprotection of the secondary amine in one reaction, saponification of the methyl ester in another, followed by coupling of the semiprotected products. The use of EDCI (*N*-(3-dimethylaminopropyl)-*N'*-ethylcarbodiimide hydrochloride) in presence of DMAP (4-dimethylaminopyridine) was found to give the best results. The resulting products were used either to synthesize a larger item of the series or deprotected at the amine end and reacted with NBD chloride as described in Figure 5.

Table 2 shows the resulting fluorescent probe set.

**Suitability of the Synthesized NBD Probes for Confocal FRAP Experiments.** With the set of synthesized probes in hand,

it was then necessary to determine if they were indeed suitable for semiquantitative confocal FRAP experiments. (i) Different concentrations of newly synthesized NBD probes in host PS were tested from  $0.5 \cdot 10^{-10} \text{ mol} \cdot \text{mg}^{-1}$  to  $5 \cdot 10^{-10} \text{ mol} \cdot \text{mg}^{-1}$ . Ratios of intensities between different concentrations are presented in Figure 6. Proportionality of intensity versus concentration implies a constant ratio. The arrow emphasizes the concentration range where intensity ratios were constant. Within this detector gain range, fluorescence intensities are proportional to probe concentration, in order to fulfill the Fick laws. The upper limit of proportionality between concentration and pixel intensity was therefore found to be with a concentration of  $5 \cdot 10^{-10} \text{ mol} \cdot \text{mg}^{-1}$  of polymer. (ii) No spotty microscopic structures were observed with any of the probes. Thus, the NBD probes can be considered as homogeneously dispersed and soluble in the polymeric matrix within the used concentration range. (iii) No fluorescence recovery from the bleached molecules was observed. Therefore, bleaching can be considered as irreversible and permanent. The recovered intensity observed is then only due to diffusion of unbleached molecules. A very different behavior was observed with fluorescein (19). (iv) Photostability at low power was found to be excessively high (less 19% after 150 successive scans). The fluorescence recovery was thus only due to diffusion of unbleached probes from the surroundings of the ROI. (v) Bleaching was found to be also efficient several planes above and below the studied confocal plane. Unbleached molecules can therefore only come from regions next to the ROI (but still within the confocal plane), leading to one-dimensional diffusion (1D).

**FRAP Kinetic Analysis.** From the recovery curve (as shown in the inset in Figure 1), Fick's equations can be applied and an apparent diffusion coefficient obtained. During FRAP experiments, one thin rectangle was bleached in order to follow diffusion over one single  $x$ -dimension (1D diffusion). Thus, Fick's second law gives eq 2, where  $t$  is time,  $C$  is concentration, and  $x$  is the position along the  $x$ -axis (3).

$$\frac{\partial C}{\partial t} = D \cdot \frac{\partial^2 C}{\partial x^2} \quad (2)$$

Numerous studies have proposed different models to estimate apparent diffusion coefficients  $D$ . They are either based on time data or have used spatially resolved profiles and their evolution over time (16, 26, 27). The mathematical developments usually fit the authors' experimental settings and cannot be automatically transposed to others. In this article, we propose a more rapid way to determine  $D$ , based on Crank's formula for 1D diffusion (3), by drawing a dimensionless nomograph (see below).

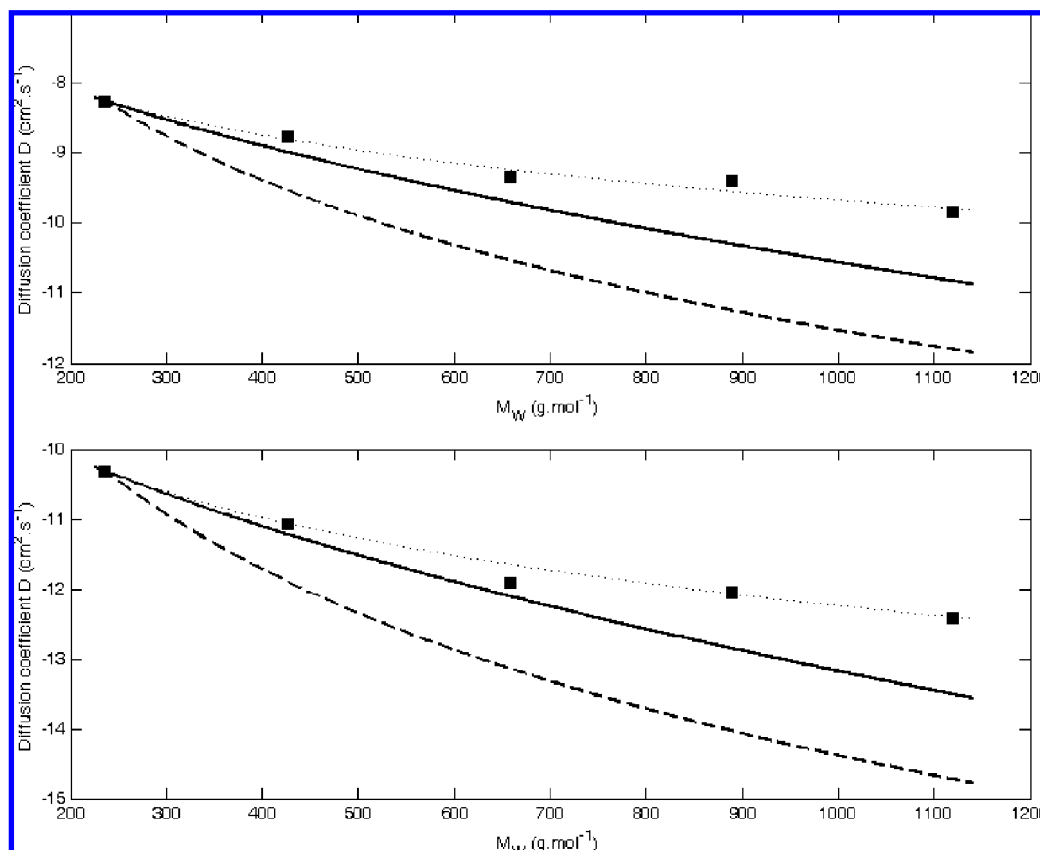
Equation is integrated for 1D diffusion and for a starting step function concentration profile to give eq 3, where  $C_\infty$  and  $C_t$  are the final concentration and the concentration at time  $t$ , respectively,  $D$  is the diffusion coefficient, and  $h$  is the half-thickness of the step function:

$$C_t = \frac{1}{2} C_\infty \left( \operatorname{erf} \left( \frac{h-x}{2\sqrt{D \cdot t}} \right) + \operatorname{erf} \left( \frac{h+x}{2\sqrt{D \cdot t}} \right) \right) \quad (3)$$

If  $z = x/h$  and  $F_0 = 2(Dt)^{1/2}/h$  as already mentioned by Vitrac (28), eq 3 gives eq 4, a simpler function, which only depends on two parameters:

$$\frac{C_t}{C_\infty} = \frac{1}{2} \left( \operatorname{erf} \left( \frac{1-z}{F_0} \right) + \operatorname{erf} \left( \frac{1+z}{F_0} \right) \right) \quad (4)$$

If integrated from  $z = -1$  (i.e.,  $x = -h$ ) to  $z = 1$  (or  $x = h$ ), this gives eq 5. Because fluorescence intensities are proportional



**Figure 9.** Experimental data and comparison with predicted values from eq 1 and ref 5. PS parameters were used for eq 1, and values from Limm and Hollifield were calculated assuming  $\alpha = 0.6$  and  $K = 1\,300$ . (Predicted values are scaled to experimental ones by normalizing to  $D_{NBDNE_b}$  in order to have the same starting value.) (■) experimental data; (—) predicted data from eq 1; (---) predicted data from Limm et Hollifield (5); the dotted lines are only visual guidelines.

to local probe concentrations, eq 5 shows the theoretical relationship between the observed percentage of fluorescence recovery and  $F_0$ , where  $I_\infty$  ( $M_\infty$ ) and  $I_t$  ( $M_t$ ) are the final fluorescence intensity (amount of diffusing species), and the fluorescence intensity (amount) at time  $t$ , respectively.

$$\% \text{ recovery} = \frac{I_t}{I_\infty} = \frac{M_t}{M_\infty} = \int_{-1}^1 \text{erf}\left(\frac{1-z}{F_0}\right) + \text{erf}\left(\frac{1+z}{F_0}\right) \cdot dz \quad (5)$$

When dealing with amorphous polymers, the infinite state is supposed to be the same as that before diffusion. Therefore, the pre-bleach intensity was used as  $I_\infty$ .

Equation 5 was used to generate normographs with Matlab. **Figure 7a** shows the relationship between the percentage of recovery and  $F_0$  for different values of  $D$ . The use of the normograph leads to quick preliminary results, allowing us to better define later experiments (i.e., ROI size and time lapse between two pictures). For more precise results, another Matlab function was written to estimate the  $F_0$  derived curve to fit experimental points, through a least-squares method, instead of reading  $D$  on the normograph (**Figure 7b**).

**FRAP Kinetic Analysis Validation Step.** Experiments reported in literature (13) have been reproduced with our methodology and technique in order to validate the FRAP kinetic analysis. Therefore, fluorescein doped solutions of sucrose were made as described in ref 13 in order to obtain a quick migration test. Champion et al. used laser interferences to create a concentration gradient instead of a CLSM. For a 68.5% sucrose solution; our method leads to a  $D$  close to literature values ( $\log_{10}D = -11.8$  versus  $-11.6 \text{ cm}^2 \cdot \text{s}^{-1}$  for

Champion et al.'s study). The difference is small and can be considered to be within the confidence interval of Champion's experiment.

**Study of  $D = f(M_w)$  in Two Model Polymers.** Our newly designed method was then applied to different systems. Two polystyrenes were chosen for preliminary tests because of their high mobility close to those of PO and their totally amorphous state. As PS500 and PS800 matrices have low  $\overline{M_w}$ , diffusion experiments for the entire set of probes were quick. As an example, the time required to collect  $D$  data range from 12 h to 60 s for  $D$  values ranging from about  $3.9 \cdot 10^{-13}$  to  $5.4 \cdot 10^{-9} \text{ cm}^2 \cdot \text{s}^{-1}$ , respectively. Results are presented in **Table 3**. As expected,  $D$  decreases when  $\overline{M_w}$  increases. Diffusion of the fluorescent probes in PS with higher  $\overline{M_w}$  is still under investigation.

**Applicability of the Fluorescent Set to Other Polymers.** Others polymers were tested as host matrix for each fluorescent NBD probe. For polyolefins (LDPE and PP), samples were not homogeneous. In samples either made through extrusion or sorption from a probe saturated solution, bright spots appeared on confocal pictures (**Figure 8**), showing that the solubility of the NBD-shaped probes in PO is too low. Dissolution of NBD probes in polyethylene oxide leads to the same phenomenon. On the contrary, samples of high molecular weight polystyrenes, polyamides, poly-(ethylene-co-vinyl acetate) (EVA), or poly-(vinyl acetate) were homogeneous. This discrimination between behavior in PO and other polymers reinforce the interest of the proposed set. Diffusion in PO, concerning food packaging, has been worked up for decades (7, 8, 12, 26), and research focuses

now on more polar polymers, which are then better barriers to migration (9, 10).

## DISCUSSION

This article deals with an alternative method able to collect  $D$  data based on the synthesis of a new set of probes with a monotone chemical structure variation as molecular weight increases over a very large range. These migrants were then used as models to investigate the  $\log D = f(M_w)$  relationship in the field of food packaging polymers. This series was specifically designed for the determination of  $D$  through confocal FRAP experiments.

**Validity and Limitations of the Presented Confocal FRAP Method.** The developed method transposes FRAP experiments in the field of polymer diffusion with the help of confocal imaging. Diffusion rates in polymers can be very low. The use of a confocal FRAP technique improves image resolution, but it also implies some limitations in the range of  $D$ , which can be monitored with this method. (i) For very low diffusing species, the size of the ROI can be shrunk to the lateral resolution of our TCS-SP2 (in bleaching mode, about 3 pixels wide). The fluorescence recovery at the end of the experiment must be 2 times higher than the noise to signal ratio. (ii) In contrast, for very mobile molecules, the limiting factor is the time between two frames (min. 0.19 s) and the ROI size. If more than 1/3 of the picture is bleached, the background no longer has a constant intensity, and fluctuations of laser illumination can no longer be corrected. At a fluorescence recovery higher than 50%, the system can no longer be considered to be under 1D diffusion because unbleached molecules from planes above and below reach the confocal plane and accelerate recovery.

**Table 4** shows the upper and lower theoretical extreme  $D$ s. The literature reports values of  $D$  only down to  $10^{-14} \text{ cm}^2 \cdot \text{s}^{-1}$  (13), but the related authors mention a maximal duration of only 1 h (29). With a modern confocal microscope and accurate motorized stages, experiments may last more than a year. The sample is then simply mounted and dismantled under the microscope for reading when necessary. In our case, we actually managed to reach  $D$  as low as  $10^{-15} \text{ cm}^2 \cdot \text{s}^{-1}$  (results not shown) with an experiment duration of about one month.

**Influence of  $M_w$  on the Probe Diffusion Coefficient.** As expected for both polymers, there is an overall decrease of  $D$  with an increase in molecular mass of the migrant (**Table 3** and **Figure 9**). Moreover, for each polymer, one single curve is required to fit all  $M_w$  data. This must be compared to values from literature. The use of alkanes as model migrants also led to aligned points. But alkanes do not realistically describe commercial additives, and their calculated  $D$  data were overestimated compared to those of real additives or underestimated if the cocrystallization phenomenon occurs (11). On the contrary, when dealing with commercial additives,  $D = f(M_w)$  data were scattered, and no significant fit was possible (7).

The presented data agrees with the general figure drawn by Dole et al. (9) for high mobility polymers. The relationship described by these authors could be therefore extended to molecular weights up to  $1100 \text{ g} \cdot \text{mol}^{-1}$  for high mobility amorphous polymers. Diffusion in PS500 seems to be less dependent on molecular mass than in polyolefins (PO).

A comparison of experimental values reported here can be made with those measured by Limm et Hollifield (5) and with those predicted from eq 1 in order to get relevant references useful to explore the available models. Predicted values are below all experimental  $D$  obtained here, but the shapes of the

curves are very similar (**Figure 9**). When increasing  $M_w$  of the migrant, predicted diffusion decrease is higher than that observed in our experiment. These models seem to integrate a higher dependence of  $D$  on  $M_w$  than observed in the tested model polymers. This peculiar behavior may come from the very low chain length of the two model PS used, that is, the relative enrichment of the chain ends and the high mobility of matrix molecules compared to common polymers, which are currently under investigation. The longest probes have  $M_w$  values higher than those of both tested matrices. Therefore, it should be kept in mind that the high mobility of matrix molecules may have a carrier effect, enhancing probe diffusion.

The two polymers used, however, validate the efficiency of the fluorescent probe set as a useful tool to collect data to improve migration models. A monotone evolution of  $D$  is obtained as a function of  $M_w$ , which will be useful for the proposal of a  $D = f(M_w)$  relationship for real commercial polymers.

**Perspectives.** Further experiments are required to complete this study of  $D = f(M_w)$  with commercial polymers. For example, experiments are planned to study the dependence of  $D$  on polymer mobility. Three different ways of changing matrix mobility will be implemented: polymer chain length, experiment temperature, and polymer plasticization.

## ACKNOWLEDGMENT

We thank the GRECI for the use of the Perkin-Elmer LS50B luminescence spectrophotometer.

**Supporting Information Available:** NBD-shaped probe synthesis and characterization. This material is available free of charge via the Internet at <http://pub.acs.org>.

## LITERATURE CITED

- Lee, K.-T.; Lee, C.-S.; Kim, D.-J. Comparison and validation of overall migration values from plastic food packaging materials obtained with different testing methods as specified in the regulations of the USA, EU and Korea or Japan. *J. Food Sci. Biotechnol.* **2002**, *11*, 654–658.
- Masaro, L.; Zhu, X. X. Physical models of diffusion for polymer solutions, gels and solids. *Prog. Polym. Sci.* **1999**, *24*, 731–775.
- Crank, J. *The Mathematics of Diffusion*, 2nd ed.; Oxford Science Publication: New York, 1975.
- Begley, T.; Castle, L.; Feigenbaum, A.; Franz, R.; Hinrichs, K.; Lickly, T.; Mercea, P.; Milana, M.; O'Brien, A.; Rebre, S.; Rijk, R.; Piringer, O. Evaluation of migration models that might be used in support of regulations for food-contact plastics. *Food Addit. Contam.* **2005**, *22*, 73–90.
- Limm, W.; Hollifield, H. C. Modelling of additive diffusion in polyolefins. *Food Addit. Contam.* **1996**, *13*, 949–967.
- European and American administrations in charge of FCM have edited practical guides for FCM petitioners. Both guides integrate the possible use of migration modelling, for normal cases. When dealing with ambiguous data, experimental data are requested. Further information can be found on respective websites (<http://www.efsa.europa.eu> and <http://www.cfsan.fda.gov>).
- Reynier, A.; Dole, P.; Feigenbaum, A. Additive diffusion coefficients in polyolefins. II. Effect of swelling and temperature on the  $D = f(M)$  correlation. *J. Appl. Polym.* **2001**, *82*, 2434–2443.
- Moisan, J.-Y. Additives diffusion in polyethylene. I. Influence of the nature of the additives. *Eur. Polym. J.* **1980**, *16*, 979–987.
- Dole, P.; Feigenbaum, A. E.; Cruz, C. D. L.; Pastorelli, S.; Paseiro, P.; Hankemeier, T.; Voulzatis, Y.; Aucejo, S.; Saillard, P.; Papaspyrides, C. Typical diffusion behaviour in packaging polymers - application to functional barriers. *Food Addit. Contam.* **2006**, *23*, 202–211.



- (10) Feigenbaum, A.; Dole, P.; Aucejo, S.; Dainelli, D.; De la Cruz Garcia, C.; Hankemeier, T.; N'Gono, Y.; Papaspyrides, C. D.; Paseiro, P.; Pastorelli, S.; Pavlidou, S.; Pennarun, P.-Y.; Saillard, P.; Vidal, L.; Vitrac, O.; Voulzatis, Y. Functional barriers - Properties and evaluation. *Food Addit. Contam.* **2005**, *22*, p 956–967.
- (11) Reynier, A.; Dole, P.; Feigenbaum, A. Prediction of worst case migration: presentation of a rigorous methodology. *Food Addit. Contam.* **1999**, *16*, 137–152.
- (12) Ferrara, G.; Bertoldo, M.; Scoponi, M.; Ciardelli, F. Diffusion coefficient and activation energy of Irganox 1010 in poly(propylene-co-ethylene) copolymers. *Polym. Degrad. Stab.* **2001**, *73*, 411–416.
- (13) Champion, D.; Hervet, H.; Blond, G.; Simatost, D. Comparison between two methods to measure translational diffusion of a small molecule at subzero temperature. *J. Agric. Food Chem.* **1995**, *43*, 2887–2891.
- (14) Axelrod, D.; Koppel, D.; Schlessinger, J.; Elson, E.; Webb, W. Mobility measurement by analysis of fluorescence photobleaching recovery kinetics. *Biophys. J.* **1976**, *16*, 1055–1069.
- (15) Smith, B. A. Photochemical methods for measuring polymer diffusion. *NATO ASI Series, Series C: Mathematical and Physical Sciences* **1986**, *182*, 397–406.
- (16) Seiffert, S.; Oppermann, W. Systematic evaluation of FRAP experiments performed in a confocal laser scanning microscope. *J. Microsc.* **2005**, *220*, 20–30.
- (17) Nazaran, P.; Bosio, V.; Jaeger, W.; Anghel, D. F.; v.Klitzing, R. Lateral mobility of polyelectrolyte chains in multilayers. *J. Phys. Chem. B* **2007**, *111*, 8572–8581.
- (18) Zucker, R. M. Quality assessment of confocal microscopy slide based systems: Performance. *Cytometry A* **2006**, *69A*, 659–676.
- (19) Braeckmans, K. Photobleaching with the Confocal Laser Scanning Microscope for Mobility Measurements and the Encoding of Microbeads. Ph.D. Thesis, Ghent University, Ghent, Belgium, 2004.
- (20) Zucker, R. M. Quality assessment of confocal microscopy slide based systems: Instability. *Cytometry A* **2006**, *69A*, 677–690.
- (21) Peinado, C.; Salvador, E. F.; Baselga, J.; Catalina, F. Fluorescent probes for monitoring the UV curing of acrylic adhesives, 1. FTIR and fluorescence in real time. *Macromol. Chem. Phys.* **2001**, *202*, 1924–1934.
- (22) Galinier, F.; Bertorelle, F.; Fery-Forgues, S. Spectrophotometric study of the incorporation of NBD probes in micelles: is a long alkyl chain on the fluorophore an advantage. *Comptes Rendus de l'Academie des Sciences - Series IIC - Chemistry* **2001**, *4*, 941–950.
- (23) Uchiyama, S.; Santa, T.; Fukushima, T.; Homma, H.; Imai, K. Effects of the substituent groups at the 4- and 7-positions on the fluorescence characteristics of benzofurazan compounds. *J. Chem. Soc., Perkin Trans. 2* **1998**, *6*, p 2165–2173.
- (24) Uchiyama, S.; Santa, T.; Okiyama, N.; Fukushima, T.; Imai, K. Fluorogenic and fluorescent labeling reagents with a benzofurazan skeleton. *Biomed. Chromatogr.* **2001**, *15*, 295–318.
- (25) Fery-Forgues, S.; Fayet, J.-P.; Lopez, A. Drastic changes in the fluorescence properties of NBD probes with the polarity of the medium: involvement of a TICT state. *J. Photochem. Photobiol. A* **1993**, *70*, 229–243.
- (26) Al-Malaika, S.; Goonetilleka, M. D. R. J.; Scott, G. Migration of 4-substituted 2-hydroxy benzophenones in low density polyethylene: Part I-Diffusion characteristics. *Polym. Degrad. Stab.* **1991**, *32*, 231–247.
- (27) Picart, C.; Mutterer, J.; Arntz, Y.; Voegel, J.-C.; Schaaf, P.; Senger, B. Application of fluorescence recovery after photobleaching to diffusion of a polyelectrolyte in a multilayer film. *Microsc. Res. Tech.* **2005**, *66*, 43–57.
- (28) Vitrac, O.; Challe, B.; Leblanc, J.-C.; Feigenbaum, A. Contamination of packaged food by substances migrating from a direct-contact plastic layer: Assessment using a generic quantitative household scale methodology. *Food Addit. Contam.* **2007**, *24*, 75–94.
- (29) Bartsch, E.; Eckert, T.; Jahr, T.; Veniaminov, A.; Sillescu, H. *Proceedings of the 8th International Symposium on Properties of Water*; Zichron Yaakov: Israel, to be published.

---

Received for review July 16, 2008. Revised manuscript received September 4, 2008. Accepted September 5, 2008. J.P. acknowledges the French Ministry of Agriculture for a Ph.D. grant.

JF802166E